

Full Paper

Patterning High Explosives at the Nanoscale

Omkar A. Nafday, Rajasekar Pitchimani, Brandon L. Weeks*

Department of Chemical Engineering, Texas Tech University, Lubbock, TX 79409 (USA)

Jason Haaheim

NanoInk Inc., 8025 Lamon Ave., Skokie, IL 60077 (USA)

DOI: 10.1002/prop.200600051

Abstract

For the first time, we have shown that spin coating and Dip pen nanolithography (DPNTM) are simple methods of preparing energetic materials such as PETN and HMX on the nanoscale, requiring no heating of the energetic material. Nanoscale patterning has been demonstrated by the DPN method while continuous thin films were produced using the spin coating method. Results are presented for preparing continuous PETN thin films of nanometer thickness by the spin coating method and for controlling the architecture of arbitrary nanoscale patterns of PETN and HMX by the DPN method. These methods are simple for patterning energetic materials and can be extended beyond PETN and HMX, opening the door for fundamental studies at the nanoscale.

Keywords: Dip Pen Nanolithography, Spin Coating, PETN, HMX, Atomic Force Microscope

1 Introduction

Preparation of nanoscale high explosive materials like pentaerythritol tetranitrate (PETN) and cyclotetramethylene tetranitramine (HMX) has been a challenging task, due to their chemical and physical properties such as decomposition at relatively low temperatures. PETN ($C_5H_8N_4O_{12}$) is a crystalline energetic material and one of the strongest known secondary high explosives, generally used as a booster for small caliber ammunition or as the explosive core of detonation cords. The properties [1–3] and X-ray diffraction characterization [4] of PETN have been extensively documented. HMX ($C_4H_8N_8O_8$) is used almost exclusively in military applications and also as a propellant. It has also been the subject of various fundamental studies [5–8]. Although these materials have been studied at the macroscopic level, very little is known about their behavior at the nanoscale. Engineering and control of energetic material properties at the nanoscale are of paramount importance when the ignition and detonation properties of high explosives (HE) are to be determined. Towards this

end, deposition of thin films at the nanoscale becomes necessary, and physical vapor deposition has been used in the past to deposit energetic materials, as demonstrated by Tappan et al. [9] and Ericson et al. [10]. Tappan et al. [11] have also demonstrated the use of semiconductor manufacturing techniques with inherent advantages of rapid throughput and integrated manufacturing. However, the nanoscale deposition of thin films of HEs presents a challenging problem because most explosives are sensitive organic molecules that decompose at relatively low temperatures, therefore thermal evaporation and sputtering methods are limited.

For the first time, we present methods for making continuous HE thin films and arbitrary HE patterns at the nanoscale. Continuous films were prepared using spin coating/spin casting. Spin coating is one of the simplest and cheapest deposition techniques in which several drops of a liquid solution are simply placed onto a spinning substrate. Centrifugal forces then spread the liquid to a uniform thickness over the entire substrate. The film's thickness is usually determined by the solution's viscosity and the rate and duration of spinning.

Arbitrary nanoscale HE patterns were produced using DPN [12], which is an application of the atomic force microscope (AFM) [13]. The AFM has the ability to image surfaces at the atomic/molecular scale in three dimensions. Studies of HE crystal properties using AFM [14, 15] have provided a better understanding of their surface reconstruction and hotspot development. The AFM generally uses a silicon nitride tip mounted on a gold coated cantilever to scan surface features. Typically, a laser signal is bounced off the back of the cantilever onto a photodetector, which is divided into four quadrants. The segmented photodetector allows for both vertical and lateral displacement of the cantilever to be recorded simultaneously. As the cantilever scans the surface, minute deviations of the piezo scanner due to surface features are registered as changes in the photodetector and a high resolution image of the surface is obtained. In the DPN method the AFM tip (radius ~ 10 – 20 nm) is coated with desired materials to be patterned (inks).

* Corresponding author; e-mail: brandon.weeks@ttu.edu

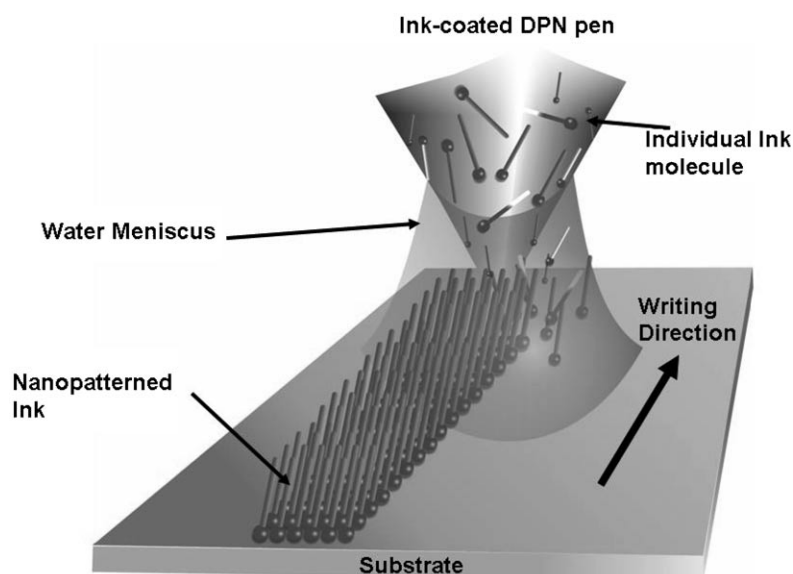


Figure 1. Schematic representation of the DPN method.

DPN has emerged favorably in comparison to other soft molecule patterning methods such as micro contact printing [16, 17] due to its high spatial resolution. Patterns can subsequently be formed at the nanoscale by moving the tip in a desired path to form dots, lines and even complex features using computer aided drafting programs [18]. The schematic representation of the DPN method using an AFM is shown in Figure 1. The water meniscus [19] formed between the tip and substrate is a proposed mode of transport of molecules from the tip and is formed by capillary condensation [20]. However, there has been no consensus in the literature [21] as to how transport of highly insoluble ink molecules can occur through the water meniscus. The DPN method has found numerous applications in patterning soluble and insoluble inks such as thiols [22, 23], dendrimers [24], gold nanostructures [25] and even magnetic nanoparticles [26].

DPN generated features, as small as 15 nm with 5 nm lateral resolution, can be patterned [27], which demonstrates the flexibility of using this method to produce complex HE structures for potential use in HE propagation studies. Since the DPN patterns have heights on the order of tenths of a nanometer, the lateral force microscopy (LFM) image is more useful in feature imaging. The LFM image (lateral twisting of the cantilever) provides contrast due to the relative friction of the differing chemical compositions. For the HE studies, silicon and mica substrates were used in the DPN method as silicon is the substrate of choice in the semi-conductor industry, which may allow for direct incorporation of HE materials into the fabrication process. Mica was also used since it is easy to obtain an atomically flat substrate for patterning.

2 Experimental

Spin coating solutions of PETN were prepared by dissolving the PETN powder in acetone (0.1 M and

0.01 M). The PETN powder was synthesized by EG&G Mound Applied Technologies, Inc. (Miamisburg, OH) and supplied by Lawrence Livermore National Laboratory (Livermore, CA). Powder samples were recrystallized out of cold acetone, and elemental analysis and Fourier transform infrared spectroscopy were used to assure purity greater than 99%. The thin films were prepared by spin coating the PETN solution onto the glass substrate at room temperature using a single wafer spin processor from Laurell Technologies Corp. (North Wales, PA). The spin speed was 2500 rpm and the spin time was 40 s. The coated film was dried in air at room temperature for 20–30 min. The film was then characterized by a Pacific Nanotechnology Inc. AFM (Santa Clara, CA) in contact mode to measure film thickness and morphology.

DPN patterning experiments were conducted at NanoInk Inc. (Skokie, IL) on two substrates: freshly cleaved mica and silicon (Si) wafer. The AFM itself was an NSCRIPTOR™ with a humidity control chamber and an air-table for vibration control. The LFM channel image was used to highlight the patterned features, as there was little topographic relief between the features and the substrate. The bare Si wafer (100) was cleaned with freshly prepared piranha solution (3 : 7 H₂O₂ : H₂SO₄ by volume) immediately before use. The mica was obtained from Ted Pella Inc. (Redding, CA) in the form of 9.9 mm diameter interleaved disks (V1 grade). The disks were freshly cleaved with sharp tweezers to give an atomically flat substrate that was immediately used to pattern on.

Milli-Q water (resistivity > 18.2 MΩ cm), prepared from a Millipore (Billerica, MA) synthesis system, was used in the chemicals preparation. Pure β-HMX crystals were prepared by the method of Siele et al. [28]. Octahydro-1,5-diacetyl-3,7-dinitro-1,3,5,7-tetrazocine was treated with 100% HNO₃ and P₂O₅ at 50 °C for 50 min, followed by quenching in ice water. Slow recrystallization from acetone yielded HMX as

colorless crystals. The HMX solution used in the DPN method was prepared by mixing 0.5 mL of anhydrous acetonitrile with ~5 mg of the HMX crystals in a glass vial to give ~33 mM solution. The vial was then sonicated to uniformly dissolve the powder. The PETN solution used in the DPN method was also prepared by mixing 0.5 mL of acetonitrile with ~5 mg of the PETN powder to give ~31 mM solution. All chemicals were used “as is” without any further modification.

Standard B type silicon nitride DPN pens were provided by NanoInk Inc. (Skokie, IL) with nominal spring constants of 0.016 N/m. The back side of the cantilever was gold coated to maximize the laser intensity. The tip was dipped into the prepared ink solution for about 10 s and then blown dry with a light spray of compressed 1–1, difluoroethane gas. This tip was then mounted onto a tip holder and was ready to pattern.

3 Results and Discussion

All experiments were conducted at room temperature (21 °C–24 °C). For DPN, the relative humidity (RH) was controlled using the environmental chamber and all images are LFM unless otherwise mentioned.

3.1 PETN Thin Films using Spin Coating

Figure 2a shows the 50 $\mu\text{m} \times 50 \mu\text{m}$ AFM topography image of the continuous thin film formed by spin coating 0.1 M PETN solution. The thickness of the film was determined by removing a portion of thin film down to the substrate, which gave a thickness of the film ~250 nm. The root mean square roughness of the film was found to be ~25 nm. Compared to the films made by physical vapor deposition [9–11], the films made by spin coating are continuous and have a thickness in the order of a few hundred nanometers, while the evaporated films are ~40 μm thick with uneven features due to the lack of a continuous mass of sufficient material [9–11]. However the film made with 0.01 M PETN solution (Figure 2b, topography image) shows a discontinuous film exhibiting both long and circular islands. The long islands have lengths of a few micrometers (3–12 μm) and their heights vary between 40 nm and 90 nm. The circular islands show heights of 100–200 nm and their diameters vary between 1 μm and 10 μm . The decrease in film thickness and continuity compared to the continuous film can be explained by the higher initial concentration (0.1 M) of the PETN solution. The increase in final film thickness with the solute concentration has been established by Meyerhofer [29]. The non-continuous films are expected due to various factors like presence of large particles on the substrate, and the long islands observed are due to evaporation of the solvent and changes in the surface tension of the fluid during spinning [30, 31]. The kind of film morphology observed was reproducible and these structures are found throughout the substrate. In addition, these

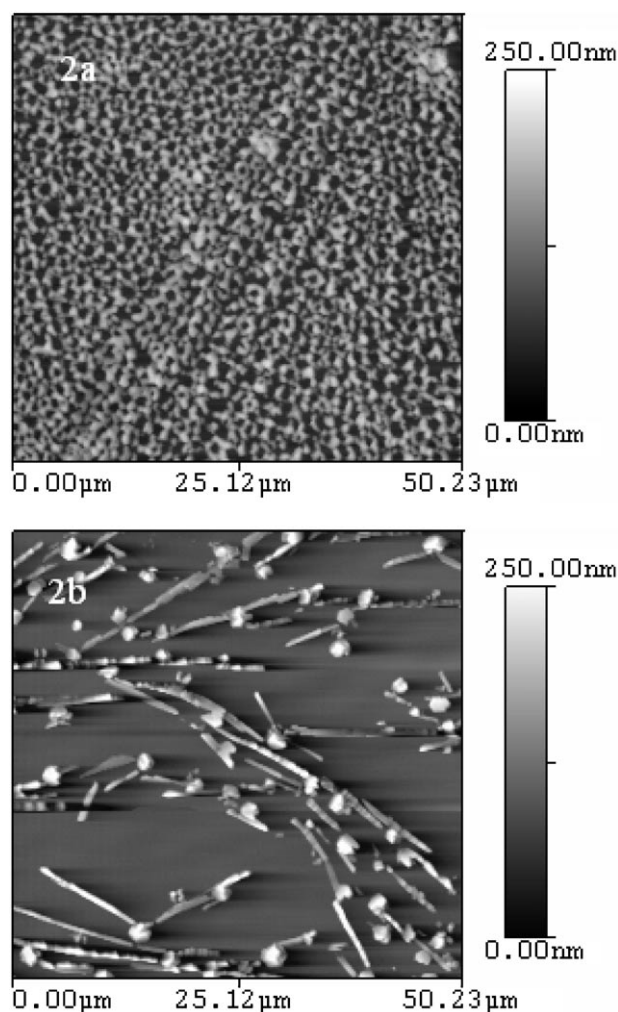


Figure 2. AFM topography image of PETN thin film by spin coating (a) 0.1 M PETN solution producing a continuous film and (b) 0.01 M PETN solution leaving islands.

structures were not observed for the film obtained from 0.1 M PETN solution. The non-continuous films are also found to be present in the films produced by spin coating 0.001 M PETN solution (not shown), with the exception that the number of islands are less. These observations indicate that the PETN concentration plays a major role in the morphology of the film. Meyerhofer [29] studied the variation of positive photoresist film thickness with the increase in spin speed (f) for different concentrations of the photoresist (dissolved in methylcellulose acetate) solution. Except for very dilute concentration, the slopes are found to be similar following $f^{-0.5}$ dependence, although there is no mention of film morphology. Apart from the concentration of the PETN solution, the surface energy of the substrate can also play a role in the final film morphology and effects of substrate surface energy and initial concentration of the PETN solution are to be studied in detail.

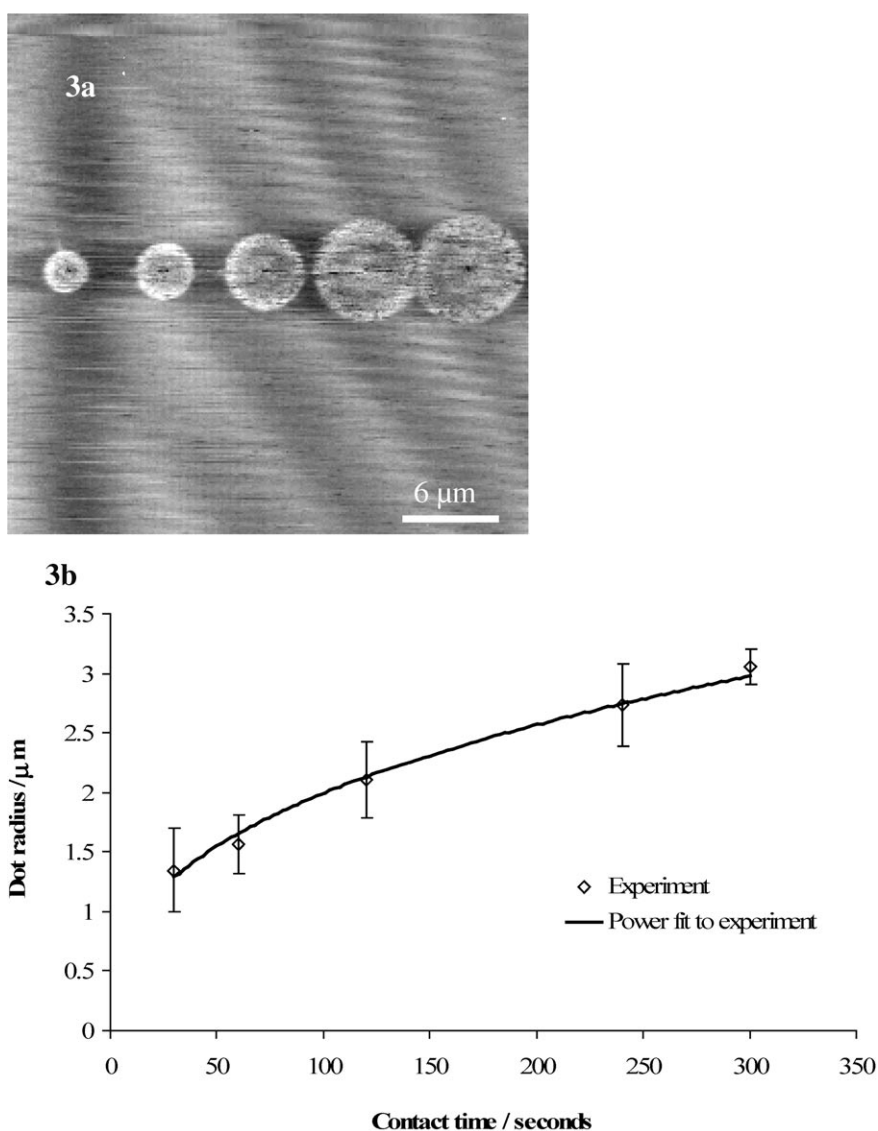


Figure 3. (a) PETN dots on mica patterned at RH 30%, 24 °C after 30 s, 60 s, 120 s, 240 s, 300 s dwell times. (b) PETN dot radii measured plotted as a function of contact time showing $t^{0.36}$ dependence.

3.2 Patterning with PETN and HMX using DPN

PETN features were patterned on cleaved mica at a range of RH from 30% to 70%. Typical PETN dots patterned on mica at RH 30% are shown in Figure 3a. The measured dot areas varied from $5.7 \mu\text{m}^2$ to $32.3 \mu\text{m}^2$ after different dwell times. The dot radius in Figure 3a followed a direct time dependent relationship ($t^{0.36}$, which is consistent with other insoluble inks [22]). The dot radii measured as a function of time are plotted in Figure 3b. PETN dots were also patterned on silicon and are discussed in the following section.

Figure 4 shows HMX features patterned on silicon and mica. HMX lines were patterned at RH 30% - 70% with line widths independent of tip speeds. HMX lines patterned on silicon at RH 40%, with different tip speeds are shown in Figure 4a, where the line width is 120 nm. HMX dots on mica were easier to pattern than on silicon and reproducible

dot features were obtained at RH 30%, 40% and 50%. Doughnut shaped HMX dots patterned on mica at RH 40% after 5–40 s dwell times with 5 s increments are shown in Figure 4b. Measured dot radii also followed a proportional dwell time dependency ($t^{0.38}$).

It is expected [32] that for slow diffusion regimes, the ink dot radius growth follows $t^{0.5}$ contact time dependence and radial growth is dependent solely on the deposition rate. This dependence assumes a constant flux of ink at the source (tip). However, a more realistic assumption is constant concentration as described by Sheehan and Whitman [22], which leads to an exponent of ~ 0.39 as observed by our experiments. It should be noted that the above sources [22, 32] modeled thiol deposition on gold, but our experiments deposited HE on non-traditional DPN substrates like mica. This validates the point that the same diffusion models can be extended to non-traditional DPN patterning such as high explosives, as demonstrated in this study.

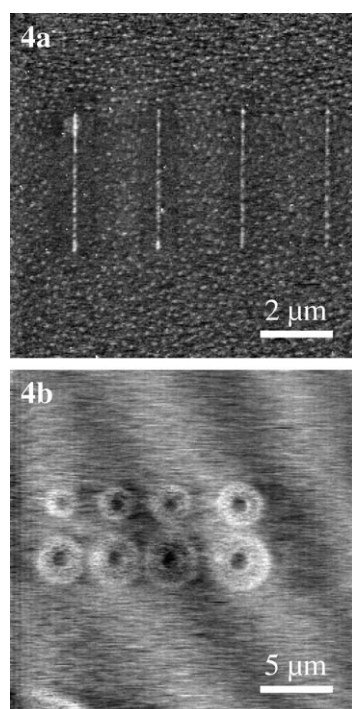


Figure 4. (a) HMX lines patterned on silicon at different tip speeds (0.05 $\mu\text{m/s}$, 0.1 $\mu\text{m/s}$, 0.2 $\mu\text{m/s}$, 0.5 $\mu\text{m/s}$, L to R). (b) HMX dots patterned on mica at RH 40% after 5–40 s dwell times with 5 s increments.

For both PETN and HMX, patterning on silicon showed no time dependence – dot sizes were similar for all contact times. This effect can be explained by the different substrate energies of silicon and mica. The relative surface energy can be measured by the contact angle of a droplet of water on the surface, where silicon has a low contact angle (forming a droplet on the substrate with a fixed size) and mica has a high contact angle (droplet wets the entire surface, spreading over time). The doughnut-shaped patterns formed on mica with HMX in Figure 4b are an indication that bulk diffusion through the meniscus may not be the primary method of transport. Rather the molecules diffuse on the outside of the meniscus, leaving hollow features on the surface [21]. These doughnut features were absent when PETN was patterned under similar conditions, suggesting that the chemical and physical properties of the HE must be considered. Molecular weight has been shown [24] to be one factor in the rate of ink transport in DPN. In this case however, the effect should be negligible since both PETN and HMX are of similar molecular weight suggesting that chemistry is the driving force in the formation of the different shapes [24].

4 Conclusions

This work demonstrates two methods of producing nanoscale energetic materials for the first time. Continuous films of nanometer scale thickness have been produced from

solutions of PETN in acetone by the spin coating method, which allows for large areas to be quickly and evenly coated with HE. We also demonstrate that high explosives can be patterned on the nanoscale using the DPN method, where complex features can be patterned with extremely high spatial resolution. These techniques are not solely limited to PETN and HMX but can be extended to any solvent soluble HE. We expect that this work will allow studies of ignition, reaction rates and manipulation of energetic materials on the nanoscale.

5 References

- [1] Y. A. Gruzdov, Y. M. Gupta, Vibrational Properties and Structure of Pentaerythritol Tetranitrate, *J. Phys. Chem. A* **2001**, *105*, 6197.
- [2] J. S. Lee, C. K. Hsu, C. L. Chang, A Study on the Thermal Decomposition Behaviors of PETN, RDX, HNS and HMX, *Thermochim. Acta* **2002**, *392–393*, 173.
- [3] Z. A. Dreger, Y. A. Gruzdov, Y. M. Gupta, Shock Wave Induced Decomposition Chemistry of Pentaerythritol Tetranitrate Single Crystals: Time-Resolved Emission Spectroscopy, *J. Phys. Chem. A* **2002**, *106(2)*, 247.
- [4] B. Olinger, P. M. Halleck, H. H. Cady, The Isothermal Linear and Volume Compression of Pentaerythritol Tetranitrate (PETN) to 10 GPa (100 kbar) and the Calculated Shock Compression, *J. Chem. Phys.* **1975**, *62(11)*, 4480.
- [5] T. R. Gibbs, A. Popolato, LASL Explosive Property Data, University of California Press, Berkeley, CA, USA **1980**.
- [6] R. S. George, H. C. Cady, R. N. Rogers, R. K. Rohwer, Solvates of Octahydro-1,3,5,7-Tetranitro-1,3,5,7-Tetrazocine (HMX), *Ind. Eng. Chem. Prod. Res. Dev.* **1965**, *4*, 209.
- [7] D. M. Hoffman, R. W. Swansiger, Partial Phase Behavior of HMX/DMSO Solutions, *Propellants, Explos., Pyrotech.* **1999**, *24*, 301.
- [8] J. C. Lynch, K. F. Myers, J. M. Brannon, J. J. Delfino, Effects of pH and Temperature on the Aqueous Solubility and Dissolution Rate of 2,4,6 TNT, RDX and HMX, *J. Chem. Eng. Data* **2001**, *46*, 1549.
- [9] A. S. Tappan, A. M. Renlund, G. T. Long, S. H. Kravitz, K. L. Ericson, W. M. Trott, M. R. Baer, Microenergetic Processing and Testing to Determine Energetic Material Properties at the Mesoscale, *12th Symposium (International) on Detonation*, San Diego, California, August 11–16, **2002**.
- [10] K. L. Ericson, R. D. Skocypec, W. M. Trott, A. M. Renlund, Development of Thin-film Samples for Examining Condensed-phase Chemical Mechanisms Affecting Combustion of Energetic Materials, *15th International Pyrotechnics Seminar*, Boulder, CO, USA, 9–13 July **1990**, 239.
- [11] A. S. Tappan, G. T. Long, A. M. Renlund, S. H. Kravitz, Microenergetic Materials - Microenergetic Materials Processing and Testing, *41st Aerospace Sciences Meeting and Exhibit*, Reno, NV, USA, 6–9 January **2003**, AIAA 2003-242.
- [12] R. D. Piner, J. Zhu, F. Xu, S. Hong, C. A. Mirkin, Dip-pen Nanolithography, *Science (Washington, DC, U.S.)* **1999**, *283*, 661.
- [13] G. Binnig, C. F. Quate, G. H. Gerber, Atomic Force Microscope, *Phys. Rev. Lett.* **1986**, *56*, 930.
- [14] B. L. Weeks, C. M. Ruddle, J. M. Zaug, D. J. Cook, Monitoring high-temperature solid-solid phase transitions of HMX with atomic force microscopy, *Ultramicroscopy* **2002**, *93*, 19.
- [15] J. Sharma, R. W. Armstrong, W. L. Elban, C. S. Coffey, H. W. Sandusky, Nanofractography of Shocked RDX Explosive Crystals with Atomic Force Microscopy, *Appl. Phys. Lett.* **2001**, *78(4)*, 457.

- [16] G. M. Whitesides, E. Ostuni, S. Takayama, X. Jiang, D. E. Ingber, Soft Lithography in Biology and Biochemistry, *Annu. Rev. Biomed. Eng.* **2001**, 3, 335.
- [17] S. R. Quake, A. Scherer, From Micro to Nanofabrication with Soft Materials, *Science (Washington, DC, U.S.)* **2000**, 290, 1536.
- [18] J. Haaheim, R. Eby, M. Nelson, J. Fragala, B. Rosner, H. Zhang, G. Athas, Dip Pen Nanolithography (DPN): Process and Instrument Performance with NanoInk's NSCRIPTOR System, *Ultramicroscopy* **2005**, 103, 117.
- [19] J. Hu, X. D. Xiao, D. F. Ogletree, M. Salmeron, Imaging the Condensation and Evaporation of Molecularly Thin Films of Water with Nanometer Resolution, *Science (Washington, DC, U.S.)* **1995**, 267, 267.
- [20] B. L. Weeks, M. W. Vaughn, J. J. DeYoreo, Direct Imaging of Meniscus Formation in Atomic Force Microscopy using Environmental Scanning Electron Microscopy, *Langmuir* **2005**, 21(18), 8096.
- [21] P. V. Schwartz, Molecular Transport from an Atomic Force Microscope Tip: A Comparative Study of Dip-Pen Nanolithography, *Langmuir* **2002**, 18, 4041.
- [22] P. E. Sheehan, L. J. Whitman, Thiol Diffusion and the Role of Humidity in Dip pen Nanolithography, *Phys. Rev. Lett.* **2002**, 88(15), 156104.
- [23] B. L. Weeks, A. Noy, A. E. Miller, J. J. De Yoreo, Effect of Dissolution Kinetics on Feature Size in Dip-Pen Nanolithography, *Phys. Rev. Lett.* **2002**, 88(25), 255505.
- [24] R. McKendry, W. T. S. Huck, B. L. Weeks, M. Fiorini, C. Abell, T. Rayment, Creating Nano-scale Patterns of Dendrimers on Silicon Surfaces with Dip-Pen Nanolithography, *Nano Lett.* **2002**, 2, 713.
- [25] H. Zhang, C. A. Mirkin, DPN-generated Nanostructures Made of Gold, Silver and Palladium, *Chem. Mater.* **2004**, 16, 1480.
- [26] L. Fu, X. Liu, Y. Zhang, V. P. Dravid, C. A. Mirkin, Nanopatterning of Hard Magnetic Nanostructures via Dip-Pen Nanolithography and a Sol-Based Ink, *Nano Lett.* **2003**, 3(6), 757.
- [27] S. H. Hong, J. Zhu, C. A. Mirkin, Multiple Ink Nanolithography: Toward a Multiple-Pen Nano-Plotter, *Science (Washington, DC, U.S.)* **1999**, 286, 523.
- [28] V. I. Siele, M. Warman, J. Leccacorci, R. W. Hutchinson, R. Motto, E. E. Gilbert, T. M. Benzinger, M. D. Coburn, R. K. Rohwer, R. K. Davey, Alternative Procedures for Preparing HMX, *Propellants, Explos., Pyrotech.* **1981**, 6(3), 67.
- [29] D. Meyerhofer, Characteristics of Resist Films Produced by Spinning, *J. Appl. Phys.* **1978**, 49, 3993.
- [30] D. P. Birnie, Rational Solvent Selection Strategies to Combat Striation Formation during Spin Coating of Thin Films, *J. Mater. Res.* **2001**, 16, 1145.
- [31] D. E. Haas, D. P. Birnie III, M. J. Zecchino, J. T. Figueroa, The Effect of Radial Position and Spin Speed on Striation Spacing in Spin on Glass Coating, *J. Mater. Sci. Lett.* **2001**, 20, 1763.
- [32] J. Jang, S. Hong, G. C. Schatz, M. A. Ratner, Self-assembly of Ink Molecules in Dip-pen Nanolithography: A Diffusion Model, *J. Chem. Phys.* **2001**, 115, 2721.

Acknowledgements

The authors acknowledge the inputs of the Chemistry team at NanoInk Inc. for useful discussions. This work was funded by the Department of Energy (RP), Office of Naval Research (OAN) and Texas Tech University Seed Funds.

(Received January 9, 2006; Ms 2006/143)